JOURNAL OF MATERIALS SCIENCE 27 (1992) 3043–3049

Magnetic field dependence of the critical current density for the bismuth-based bulk high-T_c superconductors

S. J. GUO, B. LOBERG
Department of Engineering Materials, Luleå University of Technology, S-95187 Luleå, Sweden
S. X. DOU, H. K. LIU
School of Materials Science and Engineering, University of New South Wales, PO Box 1, Kensington, NSW 2033, Australia

Three types of bismuth-based bulk samples were prepared through uniaxial pressing at room temperature, hot isostatic pressing (HIP) and drawing and rolling. Transport current properties were characterized in a steady field up to 1.12 T at 77 K ($T/T_c = 0.75$). The Josephson weak-link decoupling fields have been found to be 5 mT for the cold-pressed pellet and 30 mT for the HIPed pellet and the rolled tape. At the decoupling field the transport critical current density, J_c, drops 80% from 124 (0 T) to 29 A cm^{-2} (5 mT) for the cold-pressed pellet, 80% from 582 (0 T) to 126 A cm^{-2} (30 mT) for the HIPed sample and 50% from 6500 (0 T) to 2850 A cm^{-2} (30 mT) for the rolled tape. In the flux flow regime, where B is perpendicular to the c-axis a modified Kim's model $J_c = (\alpha/B_0)/[(1 + B/B_0)]^n$ can be used to describe the field dependence of the critical current density, J_c, in the field range 0.2–1.12 T. The effective upper critical fields were estimated to be 0.98, 1.54 and 1.94 T for the three types of samples, respectively. An adjustable range of B_{c2} for bismuth-based bulk high T_c superconductors is given. Flux shear may operate in these materials. The prediction of this pinning mechanism is yielded from fitting the equation qualitatively. When B is parallel to the c-axis, the absence of strongly intragranular flux-pinning is emphasized by the poor flux flow regime for the rolled tape sample.

1. Introduction

The problems of low transport critical current densities for most bulk high-T_c superconductors have been of great concern since they were realized. In particular, bismuth-based bulk materials, around liquid nitrogen temperature, are considered to be superconductors with some intrinsic disadvantages such as weak links, weakness of flux pinning and strong anisotropy of upper critical field [1, 2]. Many materials fabrication techniques have been used to find a way through which one expects that those disadvantages would be overcome to a large extent. Evaluations of these attempts can be obtained through investigations of the magnetic-field dependence of the transport critical current density for the resulting materials.

In the present work we characterized the field dependence of the transport critical current density, J_c, for three types of bismuth-based bulk superconductors, produced by uniaxial pressing at room temperature, hot isostatic pressing (HIP) and drawing and rolling. The J_c under a magnetic field, $B(B = \mu_0 H)$, shows a step-drop off behaviour for all three samples. When B is perpendicular to the c-axis, the weak-link decoupling field is increased by the HIPing and rolling techniques. Percolation conducting paths are enlarged by the rolling method and silver addition. In the flux flow regime, a modified Kim's model is used as a mathematical criterion for extrapolating B_{c2} of the bismuth-based bulk samples. An adjustment range for the extrapolated B_{c2} is given. A mechanism of flux shear arising from the model used is qualitatively predicted. The absence of strong intragranular flux-pinning is emphasized by the poor flux flow regime for the rolled tape sample when B is parallel to the c-axis.

2. Experimental procedure

The powders were prepared by a solid state reaction route: the powders of Bi_2O_3, PbO, $SrCO_3$, $CaCO_3$ and CuO were mixed in the ratio Bi:Pb:Sr:Ca:Cu = 1.8:0.4:2:2.2:3 by ball milling, then calcined at 800 °C for 48 h and 830 °C for 60 h, pressed into pellets and sintered at 845–850 °C for 20–120 h. The pellets were crushed and ground into powders with an average particle size of 5–10 μm. All calcination and sintering was carried out in air. X-ray powder diffraction patterns of the resulting powders show that most of the peaks correspond to those of the 110 K phase. Three materials processes were used: cold pressing, hot isostatic pressing, and drawing and rolling.

0022–2461

2.1. Cold pressing

Powders were compacted under a uniaxial pressure of 2.5 T cm^{-2} at room temperature to make a pellet with dimensions of 20 mm diameter × 2 mm. Then the green pellet was sintered at 845 °C for 48 h in air. A sintering density of 4.45 g cm^{-3}, 70% theoretical density (6.36 g cm^{-3}), was obtained. A roughly aligned surface with a thickness of 50 μm can be observed with scanning electron microscopy (SEM). The pellet shows a single but slightly broad superconducting transition with an onset temperature of 120 K, midpoint 108 K, and zero resistance at 103 K. This pellet is termed the cold-pressed sample.

2.2. Hot isostatic pressing (HIP)

A cold-pressed pellet as a precursor was encapsulated with silver plus Pyrex glass and HIPed at 650 °C under 200 MPa argon for 2 h. The density of the HIPed sample was 5.86 g cm^{-3}, 92% theoretical density. The superconducting transition midpoint temperature was 106 K and zero resistance at 103 K. This is termed the HIPed sample.

2.3. Drawing and rolling

Powders were poured into a silver tube of 10 mm outer and 8 mm inner diameter and drawn to a final outer diameter of 1 mm. The wire was then rolled into tapes with a thickness of about 0.1 mm and a width of 3 mm. The tape was then treated at 830 °C for 100 h in a mixture of oxygen and nitrogen with an oxygen partial pressure of 0.05 atm. The rolling and sintering process was repeated twice. The resulting tape shows a zero resistance of 103 K. SEM reveals excellent grain alignment with the c-axis perpendicular to the rolled surface. This sample is termed the rolled tape.

The transport currents of the cold-pressed, HIPed, and rolled samples were measured at 77 K at several constant fields up to 1.12 T. Fields both parallel and normal to the pressing direction were applied. The current was perpendicular to the field. An electric field criterion of 1 μV cm^{-1} was used for the determination of the critical transport current, I. The transport critical current density, J_c, was calculated by dividing the total current, I, by the cross-section of the sample.

3. Results and discussion

Fig. 1 shows the field dependence of J_c at 77 K and in the magnetic field perpendicular to the pressing direction. The common feature for the three bismuth-based bulk samples is that J_c shows a stepped drop off behaviour.

From a very low field of 0.05 mT, J_c decreases slightly with increasing magnetic field and then rapidly drops at about 5 mT for the cold-pressed sample and at 30 mT for the rolled tape. This is the first stepped drop off regime that extends to 30 and 100 mT for the cold-pressed and rolled samples, respectively. At fields higher than 30 or 100 mT for these two samples, plateau regions exist. The plateau extends up to 0.6 T for the rolled tape but only up to 0.1 T for the cold-pressed sample. From this plateau, J_c drops rapidly again in the second stepped drop off regime. Our experimental data are thus consistent with a model which predicts a double-step behaviour of critical current versus magnetic field in yttrium-, bismuth- and thallium-based bulk high-T_c superconductors proposed by Ekin *et al.* [3]. They describe this behaviour using three regimes: the Josephson weak-link regime (the first step), remnant percolation-path regime (the plateau region) and flux-flow regime (the second step). The discussion of magnetic-field dependence for our three types of bismuth-based bulk samples is given below.

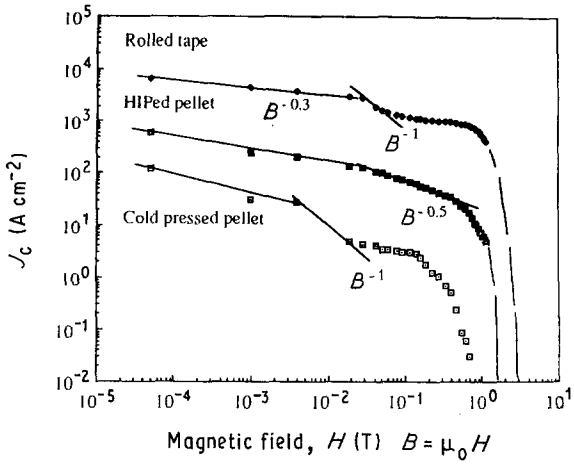

Figure 1 Characteristics of J_c for three types of bulk sample of $Bi_{1.8}Pb_{0.4}Sr_2Ca_{2.2}Cu_3O_x$ at 77 K ($T/T_c = 0.75$) in a field perpendicular to the pressing direction and to the c-axis for the rolled tape sample.

3.1. Typical stepped drop off behaviour of J_c for bismuth-based bulk material

3.1.1. The Josephson weak-link regime

(0.05 mT $\leqslant B \leqslant$ 30 mT for the cold-pressed and HIPed samples, 0.05 mT $\leqslant B \leqslant$ 100 mT for the rolled tape.) The magnetic-field behaviour of the transport critical current density is explained by a Josephson weak-link model in which the J_c data are independent of the material processing for the yttrium-based system [4, 5]. Here Fig. 1 shows that for bulk bismuth-based high-T_c superconductors, there is a similar regime (0.05 mT $\leqslant B \leqslant$ 30 mT) in which the slope of J_c is not dependent on sample fabrication techniques such as cold pressing, HIPing or rolling. In this regime the decrease in J_c appears to obey a $B^{-0.3}$ power law.

The Josephson weak-link decoupling fields (start of the drop in the J_c in the first step shown in Fig. 1) have been observed to be 5 mT for the cold-pressed pellet and 30 mT for the HIPed pellet and the rolled tape. Beyond these fields, the J_c values for all three types of samples decrease rapidly. For the magnetic-field dependence of J_c determined by weak-link decoupling, Peterson and Ekin have suggested an approximate $B^{-3/2}$ power law dependence [5]. They expect that the $B^{-3/2}$ power law could hold in multiphase materials such as bismuth-based superconductors. The present experimental data, however, show a better fit with

TABLE I Field dependence of J_c in the Josephson weak-link regime. The italicized data are the J_c values associated with the Josephson weak-link decoupling fields

Field (T)	J_c (A cm^{-2}) at 77 K		
	Cold pressed	HIPed	Rolled tape
0.00005	123.87	581.60	6496.93
0.0010	32.48	250.13	4800.41
0.0047	*28.70*	212.43	3965.53
0.0195	4.90	140.67	3164.32
0.0280	4.29	*126.13*	*2848.55*
0.0420	–	111.11	1887.62
0.0550	–	–	1646.18
0.0640	–	–	1501.32
0.0860	–	–	1404.74
0.0990	–	–	1316.95

a B^{-1} power law for the rolled tape, and possibly also for the cold-pressed pellet (see Fig. 1). This strongly supports Muller's model which gives a $(C + B)^{-1}$ dependence of J_c, where C is a constant [6]. For the HIPed sample, on the other hand, J_c is proportional to $B^{-0.5}$, which means that an intergranular pinning force density increases with the applied field between 30 and 100 mT because $F_p = JB \propto B^{-0.5}B \approx c'B^{0.5}$, where c' is a constant.

Although all three samples have a similar Josephson weak-link field dependence, the J_c levels are quite different. At the weak-link decoupling field, the J_c value of the cold-pressed pellet drops 80% from 124(0 T) to 29 A cm^{-2}, the J_c value for the HIPed sample decreases 80% from 582 to 126 A cm^{-2} and the rolled tape loses only about 50% of its zero field value from 6500 to 2850 A cm^{-2}. These different values are listed in Table I.

3.1.2. Percolation-path regime

30 mT $\leqslant B \leqslant$ 0.1 T for the cold-pressed pellet, and 100 mT $\leqslant B \leqslant$ 0.6 T for the rolled tape sample. After weak-link decoupling, the J_c characteristic does not continue to drop, but shows a plateau region instead both for the cold-pressed pellet and the rolled tape sample, as seen in Fig. 1. Such plateaus have been interpreted as the result of opening of percolation paths, which are not decoupled by the magnetic field [3]. The J_c in this plateau region is only weakly dependent on magnetic field. In the present case, the percolation-path regimes are 30 mT $\leqslant B \leqslant$ 0.1 T for the cold-pressed pellet and 100 mT $\leqslant B \leqslant$ 0.6 T for the rolled tape sample.

The slopes of the plateaus for these two samples appear to be approximately identical. This may reflect some intrinsic behaviour of the J_c for bismuth-based bulk materials, that is, the maner of opening up of percolation paths is independent of the materials processing. The width of the plateau for the rolled tape sample, however, is six times longer than that for the cold-pressed pellet. Considering the highly aligned microstructure in the rolled tape, this indicates that the amount of opened percolation paths is highly enhanced by the drawing, rolling and heat treatment. It is evident that a higher magnetic field is required to drive J_c to drop again from a wider plateau, as in the case of the rolled tape.

It is interesting to note the characteristics of J_c for the HIPed pellet. No large first step-drop off in Fig. 1 can be found. We attribute this behaviour to an improvement of the weak-link. This HIPed sample has a high density of 92% theoretical value. Densification improves the contact between the superconducting grains and grain boundaries become thinner. This leads to an increase in the weak-link decoupling field and to the disappearance of the first step in the Josephson weak-link regime. Above the decoupling field (30 mT), J_c continues to decrease. However, the rate of decrease proportional to $B^{-1/2}$ is much less than $B^{-3/2}$ dominated by weak links. This implies that the weak link is improved and that a certain number of percolation paths are opened even though the plateau is not as perfect as that of the rolled tape sample.

3.1.3. Flux-flow regime

$B \geqslant$ 0.1 T for the cold-pressed pellet, $B \geqslant$ 0.4 T for the HIPed pellet and $B \geqslant$ 0.6 T for the rolled tape. Passing through the plateau, J_c drops along the second step at the field $B \geqslant$ 0.1 T for the cold pressed pellet, $B \geqslant$ 0.4 T for the HIPed pellet and $B \geqslant$ 0.6 T for the rolled tape.

In the flux-flow regime, a modified Kim's model can fit our experimental data of the J_c versus B for all three types of bulk sample

$$J_c = \frac{\alpha/B_0}{(1 + B/B_0)^n} \quad (1)$$

where α, B_0 and n are constants, and B_0 coincides approximately with the critical field of the material. It is noticed that when $n = 1$, Equation 1 then becomes Kim's model [7]. Fig. 2a–c are the mathematical fittings, showing that the three samples give two different n values: $2 < n < 3$ for the cold-pressed sample, and $1 < n < 2$ for both the HIPed sample and the rolled tape.

3.2. Extrapolation of effective B_{c2}

The determination of B_{c2}, in general, depends on the materials processing, experimental conditions and mathematical criterion. For a conventional Type II superconductor A15 compound, a parabolic extrapolation has been established by Montgomery *et al.* [8], who define the upper critical field as the field at which the transport critical current density, J_c, reaches zero.

Here we accept this definition of B_{c2} as an effective upper critical field and use the polynomial relation in Equation 1 with $n = 2$ for extrapolating B_{c2}. Fig. 3 gives a comparison of the extrapolated B_{c2} values. The horizontal axis represents the starting reduced J_c chosen for the extrapolations. A larger J_c/J_0 means that a broader field region will be taken into account, where J_0 is the zero-field value of J_c.

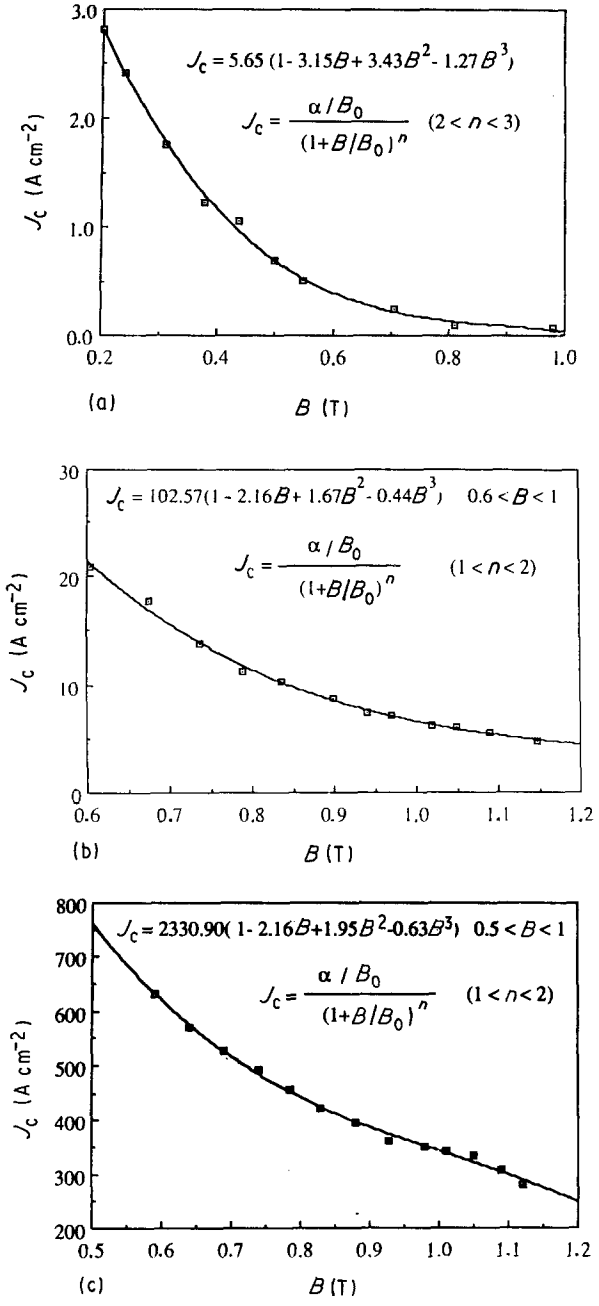

Figure 2 Field dependence of J_c obtained by fitting the data in the flux-flow regime: (a) the cold-pressed bulk sample, (b) the HIPed bulk sample; (c) the rolled tape.

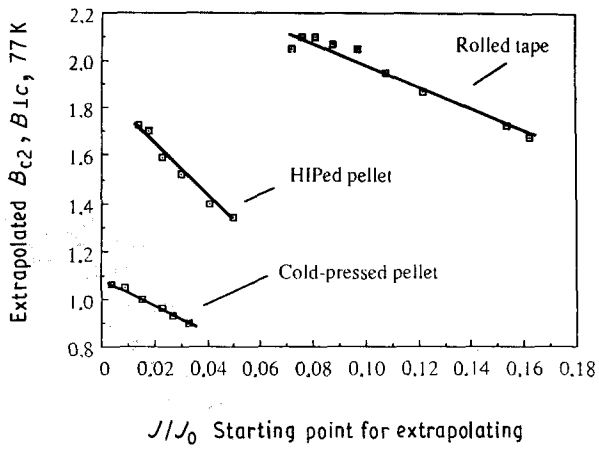

Figure 3 Comparison of the extrapolated B_{c2} for the three types of bulk sample of $Bi_{1.8}Pb_{0.4}Sr_2Ca_{2.2}Cu_3O_x$ at $T/T_c = 0.75$. J_0 is the zero-field value of J_c.

As seen in Fig. 3, the cold-pressed sample has a low $B_{c2}^{\perp}$, while the HIPed and rolled samples have higher values. On the other hand, deviations from a linear relationship can be observed for the rolled sample. These deviations, to some extent, may reveal an experimental condition dependence of the extrapolations. This can be attributed to the applied field not being high enough to drive J_c to zero. Statistics show that the deviations have a normal distribution. The extrapolated B_{c2}, deviations and the regression equations for B_{c2} versus J_c/J_0 are listed in Table II in which the average B_{c2} for the cold-pressed, HIPed, and rolled tape samples are 0.98, 1.54 and 1.94 T with 6%, 9%, and 8% S.D., respectively. Recently, Kahan shows theoretically how small changes in B_{c2} affect the evaluation of grain size, D, and the Ginzburg–Landau parameter, κ, from the scaling law for flux pinning [9]. He suggests that B_{c2} should be treated as an adjustable parameter. In the present paper, Table II may provide a range for adjusting B_{c2} for the bismuth-based bulk materials.

It is striking that the extrapolated B_{c2} of 1.94 T for the rolled tape is consistent with the results given by Palstra *et al.* [10]. They reported that the zero-resistance $B_{c2}^{\perp}$ at 76 K for the low-T_c(80 K) $Bi_2Sr_2CaCu_2O_x$ phase was only about 2 T. The lower B_{c2} values and the differences between the three types of bismuth-based bulk samples can be explained by three facts.

1. Broad superconducting transition. The cold pressed, the HIPed and the rolled tape samples show a similar broad superconducting transition of about 10 K [11, 12] even in zero field. Materials having a broad superconducting transition, in general, have a lower upper critical field which is observed in many cases even for single crystals [13, 14].

2. Highly anisotropic B_{c2}. In single crystal form B_{c2} has very strong anisotropy in particular for the bismuth system. B_{c2} anisotropies of 20–60 times have been reported for the bismuth system [15, 16], compared with an anisotropy for yttrium single crystals of only about 8 [17]. A well-aligned polycrystalline sample should have a similar anisotropy to single crystals which is reflected in a high sensitivity to the angular orientation of the grains relative to the magnetic field. The angular deviation limitation for maximum B_{c2} has been measured to be as low as 1–2° [15]. It is unlikely that the mechanical deformation processing could yield a bulk material with all grains normal to the c-axis with a variation of only about 1°–2°. Therefore, B_{c2} for the cold-pressed sample is primarily determined by a low value of B_{c2} parallel to c, whereas HIPed and rolled sample have higher values of B_{c2} due to higher degrees of alignment in these samples.

3. Local field effect. The cold-pressed bulk sample has a high porosity. Pores show an irregular cubic shape and an uneven distribution. The flux lines crossing pores should have an uneven distribution so that the local field is too high. When the current is passed, the matrix with intrinsic weak pinning cannot resist the high local Lorentz force. A low applied field is

TABLE II Statistics of the extrapolated B_{c2} values for bulk Bi–Pb–Sr–Ca–Cu–O samples at $T/T_c = 0.75$, B ⊥ C for the rolled tape sample

$B_{c2} = a + b(J_c/J_0)$	a	b	J_c/J_0 ($\times 10^{-2}$)	B_{c2} (average)	S.D.
Cold-pressed	1.09	− 5.38	4.0–3.3	0.98	0.06
HIP-ed	1.76	− 8.27	1.2–5.0	1.54	0.14
Rolled tape	2.37	− 4.12	7.2–1.6	1.94	0.16

Note: the adjustable range of B_{c2} is given by the regression equation of $B_{c2} = a + b(J_c/J_0)$ with various J_c/J_0 values.

strong enough to put J_c near zero. Thus the extrapolated B_{c2} should be lower. The HIPed sample has a higher density and the field distribution is improved. Correspondingly, the extrapolated B_{c2} is higher.

Now we check the extrapolated B_{c2} values through fitting the normalized pinning force density versus reduced field by a scaling law. Recalling Kim's model, the constant B_0 is considered to be (1) the upper critical field by Dew-Hughes, who pointed out that when $B > B_0$, JB is constant [18], and (2) the local field by Alford *et al.* [19] for discussing the self-field effect. Here we are trying to assign the effective upper critical field as B_0. Then the extrapolation equation used will give rise to a qualitative prediction for the pinning mechanism operating in the present materials.

As seen in Fig. 2b and c, the modified Kim's model leads to the extrapolation equations near

$$J_c = \frac{\alpha}{B_0}(1 - 2B + 2B^2 - 0.5B^3) \quad B < 1 \qquad (2)$$

Substituting B by b, $b = B/B_{c2}$ and $b \ll 1$, this equation should hold and becomes

$$J_c = \frac{\alpha'}{B_{c2}}(1 - 2b + 2b^2 - 0.5b^3) \qquad (3)$$

Because $b \ll 1$ in a low field, the high order term of b^3 can be neglected. Simplifying gives

$$J_c = \frac{\alpha'}{B_{c2}}[(1 - b)^2 + b^2] \qquad (4)$$

Neglecting b^2 compared to $(1 - b)^2$, we have

$$J_c = \frac{\alpha'}{B_{c2}}(1 - b)^2 \qquad (5)$$

Multiply both sides by B. Then a field dependence of the pinning force density, F_p, is obtained

$$F_p = J_c B = \alpha' b(1 - b)^2 \qquad (6)$$

This is just a common form of the scaling law from the flux line shear mechanism.

Fig. 4 is a plot of $F_p/F_{p\,max}$ against the reduced induction b for the HIPed sample. The experimental data are fitted by Equation 6 with two extrapolated B_{c2} values 1.34 and 1.73 T, which were calculated from the regression equation for the HIPed sample in Table II when $J/J_c = 0.05$ or 0.014. In this adjustable range both the experimental data and the calculation with $B_{c2} = 1.34$ T give the peak F_p at $b = 0.29$. The fitting in the lower field range is satisfactory. However, the calculation with $B_{c2} = 1.73$, although the variation is

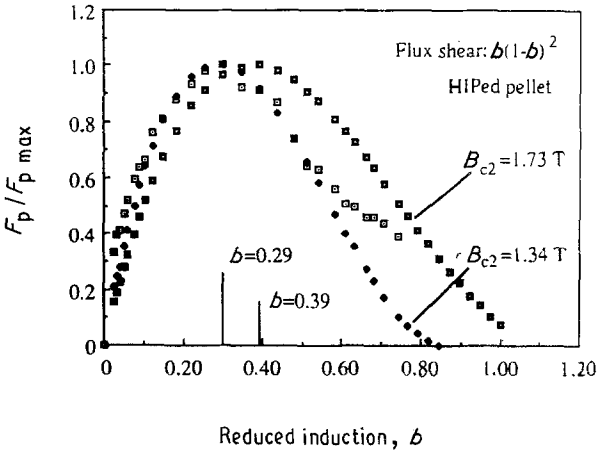

Figure 4 Plot of the fit of experimental $F_p/F_{p\,max}$ with a flux-shear scaling law where F_p is proportional to $b(1 - b)^2$ for the HIPed sample. The peak occurs at $b = 0.29$ both in the experimental and in the calculated curve, when the extrapolated value of $B_{c2} = 1.34$ T is used. The effect of an adjustment range of 1.34 T < B_{c2} < 1.73 T can be observed. For example, when $B_{c2} = 1.73$ T is used, the maximum peak occurs at $b = 0.39$.

well within the limits of error for regression analysis, moves the peak to $b = 0.39$. This should affect the estimation of some parameters from further argument with the scaling law.

For flux line shear, Campbell and Evetts [20] illustrated the field dependence of $b(1 - b)^2$ giving $b = 0.33$. The adjustable range given here covers this typical value. Fig. 4, thus, shows the applicability of the extrapolated B_{c2} and indicates that a good fit in the total field range will be obtained if a proper mathematical formula for the flux shear mechanism is chosen.

3.3. Absence of strong intragranular flux-pinning

Fig. 5 shows the magnetic-field dependence of J_c for three samples in the field of B parallel to c at 77 K. Comparing with the case of B perpendicular to c in Fig. 1, the behaviour of J_c when B parallel to c shows a strong material processing dependence. For the cold-pressed pellet, J_c decreases from 124 A cm^{-2} at 0.05 mT to 3.62 A cm^{-2} at 30 mT and then drops continuously down to 1.82 A cm^{-2} at 0.05 T. One cannot find a weak-link decoupling field, percolation-path regime or flux-flow regime, indicating that J_c is completely controlled by the weak-link.

For the HIPed sample, the J_c curve remains approximately identical to that when B is perpendicular

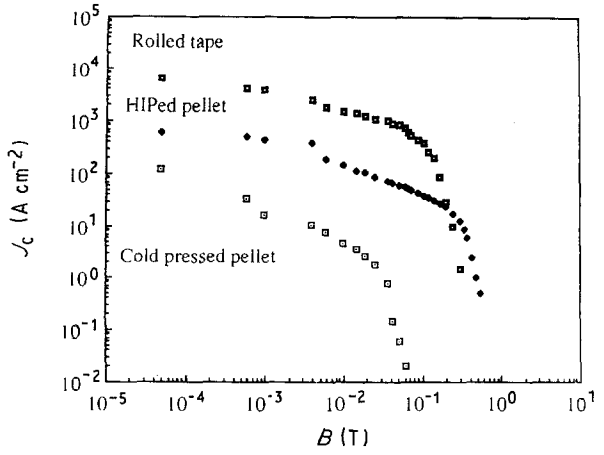

Figure 5 Characteristics of J_c for three types of bulk sample of $Bi_{1.8}Pb_{0.4}Sr_2Ca_{2.2}Cu_3O_x$ at 77 K ($T/T_c = 0.75$) in a field parallel to the pressing direction and to the c-axis for the rolled tape sample.

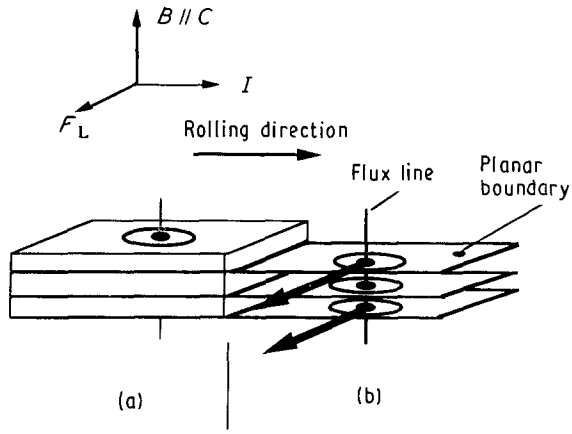

Figure 6 Schematic illustration of flux-flow within a planar boundary parallel to the Lorentz force. (a) Pinning in the grain, (b) without pinning in the grain, resulting in flux-flow.

to c. The decoupling field is 30 mT at which J_c is 76 A cm^{-2} and then drops to zero at 0.6 T.

For the rolled tape sample, the J_c curve changes from a double-stepped drop off into a one-step drop off like that of the cold-pressed pellet. This indicates that when B is parallel to c, i.e. perpendicular to the rolled surface, J_c is dominated by the weak-link Josephson junction between the superconducting grains in the a–b plane. The difference is that the rolled tape has a higher J_c value, for example, 1080 A cm^{-2} at 30 mT and 597 A cm^{-2} at 0.1 T whereas J_c is nearly zero for a polycrystalline bulk pellet.

A more important observation, as shown in Fig. 5, is that J_c for the rolled tape sample decreases more rapidly than J_c does for the HIPed sample above 50 mT. This occurs in the flux flow regime, implying that the resistance to flux-flow in the rolled tape is lower than in a denser HIPed pellet when B is parallel to c. The question arises of why the aligned microstructure in the rolled tape exhibits such a weak flux pinning characteristics.

Fig. 6 gives a schematic explanation. When B is parallel to c, magnetic flux lines easily enter the superconductor through the aligned planar boundaries with a larger area. The transport current perpendicular to B in the a–b plane leads to a Lorentz force parallel to the planar boundaries. If there is a strong flux-pinning in the grains, as shown in Fig. 6a, flux flow will be resisted. Weak flux pinning in the grains will result in considerable flux flow, as shown in Fig. 6b. The J_c behaviour illustrated in Fig. 5 for the rolled tape proves the pinning characteristics of the rolled tape to be the latter, indicating the absence of strong intragranular flux-pinning.

The randomly oriented grain boundaries in a polycrystalline bulk superconductor may have some flux-pinning effect resulting from the boundaries which are perpendicular to the Lorentz force. The aligned planar boundaries parallel to the Lorentz force in the rolled tape completely lose their pinning ability and provide a region where the flux lines can travel without any pinning. Thus the rapid drop in J_c for the rolled tape when B is parallel to c can be understood. Moreover it makes sense that the urgent task to enhance J_c for the superconducting wire or tape is by increasing the intragranular flux pinning to a larger extent. A combination of grain alignment and orientation of desirable planar defects may be a valuable means of striving towards high J_c in the bismuth-based materials [21].

4. Conclusion

The transport critical current density for bulk bismuth-based high-T_c superconductors shows a stepped drop off behaviour under a magnetic field. A weak link, to some extent, can be improved by material fabrication techniques such as HIPing or drawing–rolling and sintering. When B is perpendicular to c, a modified Kim's model can describe the field dependence of the critical current density for three types of bismuth-based bulk samples in the flux-flow regime. Three different extrapolated B_{c2} values have been found. An adjustable range of B_{c2} for bismuth-based bulk materials is given. Flux shear may operate in the present samples. Any essential enhancement of the transport critical current density relies on the improvement of the weak link and the presence of pinning centres in the grains.

Acknowledgements

The authors thank the Swedish National Board for Technical Development, Metal Manufactures Ltd, and the Commonwealth Department of Industry, Technology and Commerce, Australia, for financial support.

References

1. E. M. GYORGY, R. B. van DOVER, S. JIN, R. C. SHERWOOD, L. F. SCHNEEMEYER, T. H. TIEFEL and J. V. WASZCZAK, *Appl. Phys. Lett.* **53** (1988) 2223.
2. D. LUNDY, J. RITTER, L. J. SWARTZENDRUBER, R. D. SHULL and L. H. BENNETT, *J. Superconduct.* **2** (1989) 273.

3. J. W. EKIN, T. M. LARSON, A. M. HERMANN, Z. Z. SHENG, K. TOGANO and H. KUMAKURA, *Physica C* **160** (1989) 489.
4. R. L. PETERSON and J. W. EKIN, *Phys. Rev.* **B37** (1988) 9848.
5. *Idem, Physica C* **157** (1989) 325.
6. K.-H. MULLER, J. C. MacFARLANE and R. DRIVER, *ibid.* **158** (1989) 69.
7. Y. B. KIM, C. F. HEMPSTEAD and A. R. STRNAD, *Phys. Rev.* **129** (1963) 528.
8. D. B. MONTGOMERY and W. SAMPSON, *Appl. Phys. Lett.* **6** (1965) 108.
9. A. KAHAN, *Cryogenics* **30** (1990) 678.
10. T. T. M. PALSTRA, B. BATLOGG, L. F. SCHNEEMEYER, R. B. van DOVER and J. V. WASZCZAK, *Phys. Rev.* **B38** (1988) 5102.
11. S. X. DOU, H. K. LIU, M. H. APPERLY, K. H. SONG, C. C. SORRELL, K. E. EASTERLING, J. NISKA and S. J. GUO, *Physica C* **167** (1990) 525.
12. S. X. DOU, H. K. LIU, S. J. GUO, K. E. EASTERLING and J. MIKAEL, *Supercond. Sci. Technol.* **2** (1988) 274.
13. T. T. M. PALSTRA, B. BATLOGG, R. B. van DOVER, L. F. SCHNEEMEYER and J. V. WASZCZAK, *Appl. Phys. Lett.* **54** (1988) 763.
14. T. MATSUSHITA and B. NI, *Physica C* **166** (1990) 423.
15. M. J. NAUGHTON, R. C. YU, P. K. DAVIES, J. E. FISCHER, R. V. CHAMBERLIN, Z. Z. WANG, T. W. JING, N. P. ONG and P. M. CHAIKIN, *Phys. Rev.* **B38** (1988) 9280.
16. Y. KOIKE, T. NAKANOMYO and T. FUKASE, *Jpn. J. Appl. Phys.* **27** (1988) L841.
17. G. W. CRABTREE, W. K. KWOK, U. WELP, R. BURRIEL, H. CLAUS, K. G. VANDERVOORT and J. Z. LIU, *J. Magn. Magn. Mater.* **76, 77** (1989) 547.
18. D. DEW-HUGHES, *Mater. Sci. Engng* **1** (1966) 2.
19. N. McN. ALFORD, T. W. BUTTON, D. H. JONES, J. D. BIRCHALL, C. E. GOUGH and S. J. DENN, *Cryogenic* **29** (1990) 434.
20. A. M. CAMPBELL and J. E. EVETTS, *Adv. Phys.* **21** (1972) 199.
21. S. X. DOU, H. K. LIU, J. WANG, M. H. APPERLY, C. C. SORRELL, S. J. GUO, B. LOBERG and K. E. EASTERLING, *Physica C* **172** (1990) 63.

Received 6 February
and accepted 14 June 1991